Materials and Design 31 (2010) 3599–3604

Contents lists available at ScienceDirect

Materials and Design

journal homepage: www.elsevier.com/locate/matdes

Effect of hot working on flow behavior of Ti–6Al–4V alloy in single phase and two phase regions

A. Momeni [a,*], S.M. Abbasi [b]

[a] Department of Mining and Metallurgy, AmirKabir University of Technology, Tehran, Iran
[b] KNT University of Technology, Tehran, Iran

ARTICLE INFO

Article history:
Received 22 September 2009
Accepted 26 January 2010
Available online 21 February 2010

Keywords:
Ti–6Al–4V
Hot compression
Flow stress
Characteristic strain

ABSTRACT

Hot deformation behavior of the alloy Ti–6Al–4V was investigated via conducting hot compression tests at temperatures of 800–1150 °C and at strain rates, ranging from 0.001 s^{-1} to 1 s^{-1}, at an interval of an order of magnitude. The apparent differences of flow stress curves obtained in dual phase $\alpha + \beta$ and single phase β regions were analyzed in term of different dependence of flow stress to temperature and strain rate and different microstructural evolutions. The values of strain rate sensitivity and apparent activation energy were obtained respectively as 0.20 and 530 kJ/mol for two phase microstructure. However, for single phase β microstructure they were approximated as 0.19 and 376 kJ/mol, respectively. It was found that in two phase region the values of strains corresponding to peak point, ε_p, and the highest rate of flow softening, ε^*, are almost independent to Zenner–Hollomon parameter. In single phase region, ε_p and ε^* exhibited a direct relationship to Z parameter and the corresponding empirical equations were proposed.

1. Introduction

The desired mechanical characteristics and good corrosion resistance in most of titanium alloys are concomitantly satisfied when a precise control is considered on processing route and thereby on microstructure. Particularly, the influence of resulting microstructure upon the mechanical properties and the corrosion behavior in different alloys were widely discussed by other researchers [1–4].

The Ti–6Al–4V alloy is the most applicable among titanium alloys due to its excellent mechanical properties as well as good corrosion resistance. The use of this alloy is particularly attractive in aerospace and biomaterials industry [5]. Hot deformation in different actual industrial processes such as hot forging or rolling is extensively used for manufacturing of both semi-finished and finished products of this alloy. The previous researchers have tried to investigate the microstructural and mechanical behaviors of this alloy under hot working conditions by physical and mathematical simulative techniques. Seshacharyulu et al. [6] were studied the hot deformation behavior and damage mechanisms in an extra low interstitial (ELI) grade Ti–6Al–4V. Other studies have got involved in the effect of texture or morphology of α-phase in $(\alpha + \beta)$ microstructure on the hot deformation characteristics of the alloy [7–10].

Tracking microstructural evolutions and mechanical properties, many investigations have done in two phase domain to analyze the restoration mechanisms [11–15]. Irrespective of morphology of constituent phases at dual phase state, globularization of α-phase during hot deformation is the major microstructural phenomenon which is considered to be responsible for flow softening. Although, less attention have paid to the hot working of the Ti–6Al–4V alloy in single phase β region, beyond β transus, it is proposed the likely occurrence of dynamic and metadynamic recrystallizations (DRX and MDRX) in this phase [16]. Dealing with industrial hot working processes, Hu and Dean [17] probed the hot forging response of the Ti–6Al–4V alloy for production of near to net-shape products and Park et al. [18] analyzed deformation stability in hot forging using a processing map. Moreover, Kim et al. [19] analyzed the high temperature deformation mechanisms of a single phase α titanium alloy as well as an $\alpha + \beta$ two phase one by an inelastic-deformation theory. More recently, Li and Zhang [20] investigated the Ti–6Al–4V alloy in hot compression and proposed the effect of hydrogen content on hot deformation characteristics.

The aim of present research is to investigate the behavior of the Ti–6Al–4V alloy under straining via hot compression at both single β-phase and dual phase $(\alpha + \beta)$ regions. Even though resembling other previous investigations, in this study mechanical analysis have assigned, the attention was particularly paid to apparent features of flow behavior and characteristic points in order to make more exact and reliable results.

* Corresponding author. Tel.: +98 9123349007.
E-mail address: ammomeni@aut.ac.ir (A. Momeni).

0261-3069/$ - see front matter © 2010 Elsevier Ltd. All rights reserved.
doi:10.1016/j.matdes.2010.01.060

2. Experimental procedures

The studied Ti–6Al–4V alloy with the composition of 6.66 wt.% Al, 5.13 wt.% V, 0.21 wt.% Fe, 0.03 wt.% Mo, 0.02 wt.% Mn, 0.02 wt.% Si and the balance of Ti was received as wrought strip of 12 mm thick. The β transus temperature was measured to be approximately 980 °C by thermal dilatation method. The vanadium content of the studied alloy was about 1% higher than the standard average. As vanadium is a β stabilizer element [21], the β transus was about 20 °C lower than that was measured by previous investigators [10–12].

Cylindrical compression samples of 15 mm height and 10 mm diameter were prepared with the axis along the rolling direction of the as-received plate according to the ASTM E209 standard. Dimensions of the specimens were chosen in a manner to minimize the buckling phenomena, and also to ensure appropriate rigidity in the testing system. Concentric grooves of 0.5 mm depth were made on the both surfaces contacting the anvils to keep lubricant material and help to reduce friction. A 1 mm 45° chamfer was machined on the specimens edges to avoid fold-over of the material during the early stages of hot deformation. A small hole of 0.8 mm diameter and 5 mm depth was drilled at mid height of the specimens for embedding a thermocouple used for the measurement of real temperature of the specimens. Graphite powder was used to reduce the friction and therefore minimizing the sample barreling. The temperature of the specimens was monitored using a chromel–alumel thermocouple. An INSTRON 8502 testing machine equipped with a fully digital and computerized control furnace was employed to perform hot compression tests under constant strain rates, ranging from 10^{-3} s^{-1} to 1 s^{-1} at an interval of an order of magnitude and at temperatures of 800 °C, 850 °C, 900 °C, 950 °C, 1000 °C, 1025 °C, 1050 °C and 1075 °C.

3. Results and discussion

Typical flow stress curves obtained at low and high temperatures, i.e. in two phase α + β and single phase β regions, are shown in Fig. 1. It is well known and also clearly seen here that flow stress level actually increases with strain rate and descends with temperature [9,12].

The apparent discrepancies between the flow curves obtained at temperatures below and above β transus, i.e. in two phase and in single phase regions respectively, reflect the different microstructural evolutions and restoration processes which are dominant during individual regime. In the two phase region of α + β, the flow stress increases rapidly and reaches a sharp summit followed by a steep downfall up to a plateau. This behavior is more obvious at higher strain rates. Otherwise, in the single phase β region, the rate of work hardening is almost lower than that in the two phase region and the flow curve degrades more gently leaving a blunt peak. In addition, more oscillatory appearance of flow curve at higher temperatures can be likely attributed to the occurrence of dynamic recrystallization in β [6,8,9,15].

Fig. 2 demonstrates the typical microstructures of hot deformed specimens at different temperatures. Fig. 2a and b exhibits the effect of deformation temperature in two phase regime on resulting microstructure. The globularized morphology of α in a matrix of transformed β is the characteristic feature of both micrographs. However, it is apparent that the progress of globularization process diminishes with decrease in temperature. The lower volume fraction of α at higher temperatures which is the result of α to β transformation degrades the softening effect of globularization and leads to more sluggish subsidence of flow stress. In single phase β regime, Fig. 2c and d shows dynamically recrystallized β grains surrounded by irregular boundaries. At higher deformation tem-

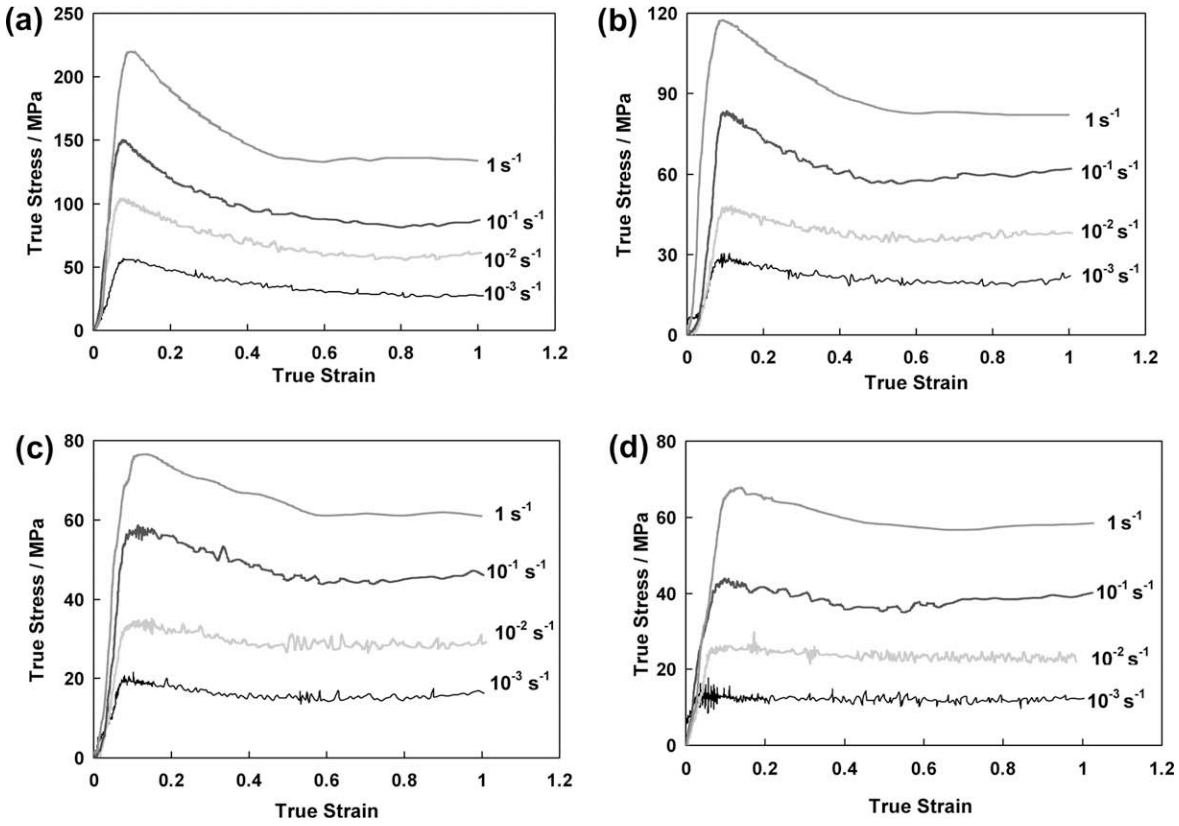

Fig. 1. True stress–true strain curves obtained from hot compression tests at different strain rates and temperatures of (a) 900 °C, (b) 950 °C, (c) 1000 °C and (d) 1050 °C.

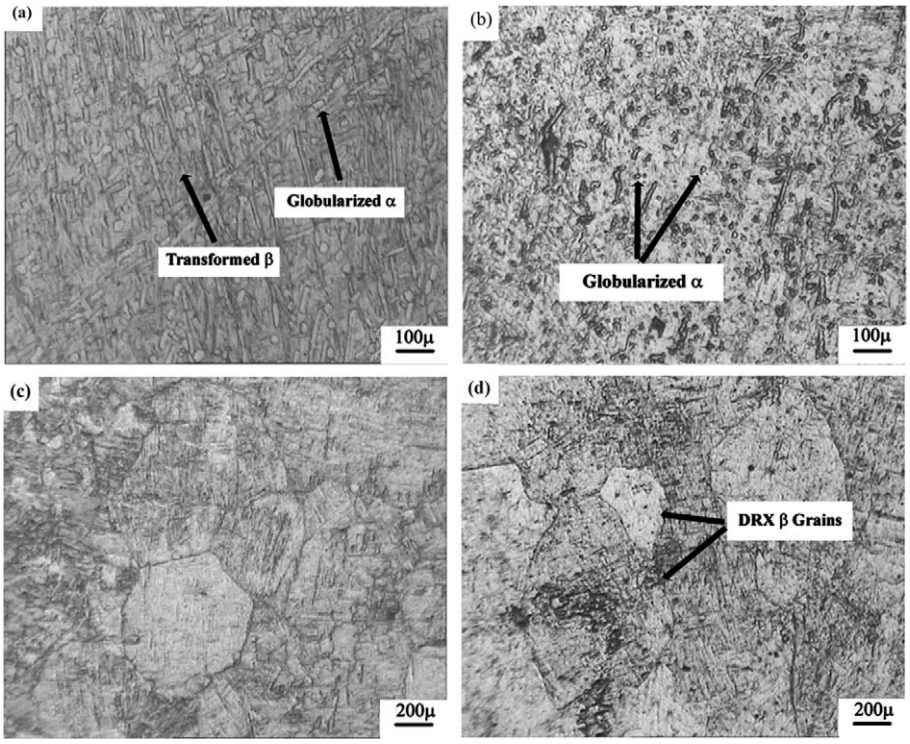

Fig. 2. Microstructure of deformed samples at strain rate of 0.001 s^{-1} and different temperatures: (a) 900 °C, (b) 950 °C, (c) 1000 °C and (d) 1050 °C.

perature, where DRX occurs more feasibly, β grains are more distinguishable and a bit coarser.

Irrespective of dominant microstructural phenomena or restoration process during hot deformation, determination of the relation between strain and stress of peak (ε_p and σ_p) and processing variables, i.e. T and $\dot{\varepsilon}$, is of great importance. The effects of temperature and strain rate are incorporated into the very well-known Zenner–Hollomon parameter, Z, given by [22]:

$$Z = \dot{\varepsilon}\exp(Q/RT) \tag{1}$$

where Q and R denote apparent activation energy and gas constant, respectively. In order to determine the relationship between either ε_p or σ_p and temperature compensated strain rate, Z, the first step is to determine the values of apparent activation energy in both two phase and single phase regions. The apparent activation energy describes the activation barrier that atoms need to conquer to follow the deformation procedure. In this respect, the temperature and strain rate dependence of flow stress in hot deformation condition is generally expressed via a kinetic equation as follows [14]:

$$\dot{\varepsilon} = A\sigma^n\exp(-Q/RT) \tag{2}$$

where A is a constant frequency factor, σ is flow stress and n is stress exponent which is defined as the reverse of strain rate sensitivity exponent, m. From Eq. (2) the strain rate sensitivity and the apparent activation energy are given as follows [11,15,23]:

$$m = \frac{\partial \ln\sigma}{\partial \ln\dot{\varepsilon}} \tag{3}$$

$$Q = \frac{R}{m}\cdot\frac{\partial \ln\sigma}{\partial(1/T)} \tag{4}$$

Fig. 3 indicates the variation of flow stress with strain rate at the strain of 0.5. As it is evident the average slope, i.e. the m value, is approximately the same for both microstructural regions. The average value of m can be introduced respectively as 0.20 and 0.19 for α + β and β. According to the inverse relationship between m and n the average values of the later are obtained 5.0 and 5.1 for α + β and β, respectively. The values introduced for m and n in this research are in good agreement with other investigations [16,17].

Fig. 4 exhibits the variation of flow stress with inverse of deformation temperature in both microstructural regions. The different slopes obtained in different sides of the β transus declare that flow stresses in α + β two phase region are much more temperature dependent than in single phase β region. It may be concluded that the dominant microstructural evolution during hot deformation of β is likely dynamic recrystallization during which flow stress shows less dependency on temperature. Otherwise, the very temperature-dependent flow stress in two phase region reflects the occurrence of a phase transformation like globularization.

As it is well documented, the occurrence of dynamic phase transformations, which is so-called strain induced transformation (SIT), before dynamic restoration processes may retard or even inhibit the later process. In this case, the stored energy in the micro-

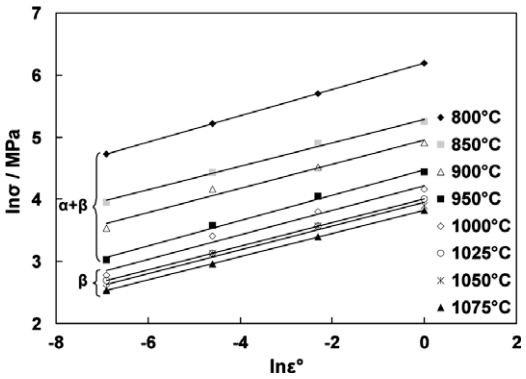

Fig. 3. Variation of flow stress with strain rate in both two phase α + β region and single phase β region at the strain of 0.5.

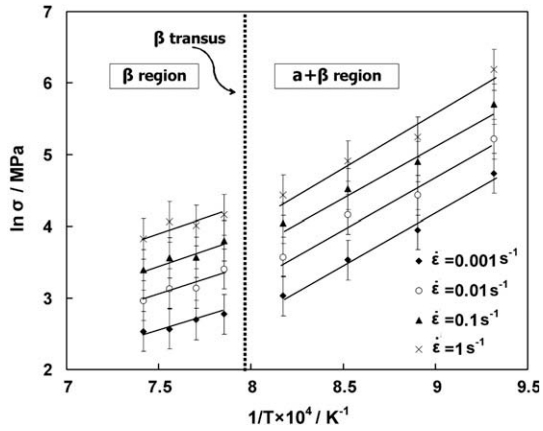

Fig. 4. Variation of flow stress with deformation temperature in both two phase α + β region and single phase β region at the strain of 0.5.

structure of deformed material is consumed by the SIT process and therefore it can be introduced as a pseudo-restoration process.

The obtained values of m and $\partial \ln \sigma / \partial(1/T)$ were used according to Eqs. (3) and (4) to calculate the apparent activation energy of α + β and single phase β regions as 530 kJ/mol and 376 kJ/mol, respectively. The existence of more active slip systems and higher diffusion coefficient in bcc structure of β in comparison to hcp structure of α, are the main reasons for more feasibility of deformation and lower apparent activation energy in β-phase [24]. The obtained values for the activation energy are in good agreement with the results of Seshacharyulu et al. [9] and Bruschi et al. [11] but not with those of Ding et al. [16] and Tangerila et al. [24]. It is well understood that activation energy actually depends on chemical composition and microstructure. Tangerila et al. [24] had used an ELI alloy having lower content of vanadium and the primary β grain size in the research conducted by Ding et al. [16] had been 1100 μm which was very larger than 150–250 μm in this investigation.

The relation between the temperature compensated strain rate parameter, Z, and flow stress in hot deformation condition is well established via the constitutive equation of hyperbolic sine function proposed by Sellars et al. [25] as follows:

$$Z = A[\sinh(A'\sigma)]^n \tag{5}$$

where A, A' and n denote frequency factor, material constant and constant stress exponent, respectively. From Eqs. (1) and (5), A' is calculated as follows [7]:

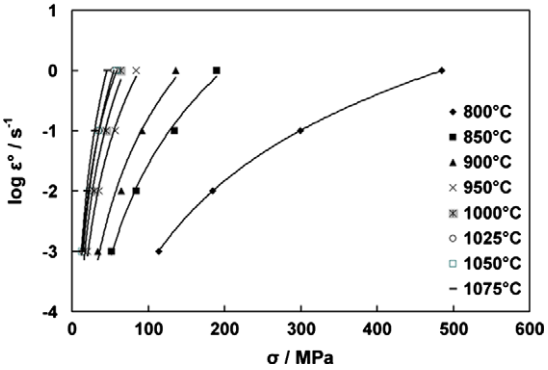

Fig. 5. Variation of strain rate with flow stress at different deformation temperature for determination of α parameter according to Eq. (6).

$$A' = \left(\frac{2.303}{n}\right)\left(\frac{\partial(\log \dot{\varepsilon})}{\partial \sigma}\right) \tag{6}$$

Fig. 5 exhibits the curves of $\log \dot{\varepsilon}$ versus flow stress at different deformation temperatures. Putting the average slope in Eq. (6), the average value of A' parameter is estimated to be 0.007.

The validity of hyperbolic sine function can be appraised by studying the variation of $\ln Z$ versus $\ln[\sinh(A'\sigma)]$ in Fig. 6 and the slope is therefore introduced as the stress exponent, n. The esti-

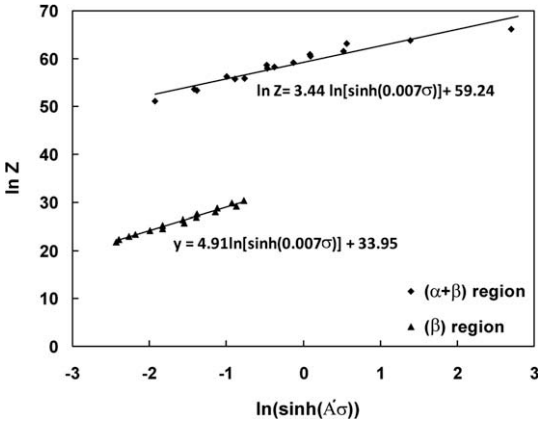

Fig. 6. The evaluation of hyperbolic sine law in term of the relationship between flow stress and Z parameter during hot deformation of alloy Ti–6Al–4 V in different microstructural regimes.

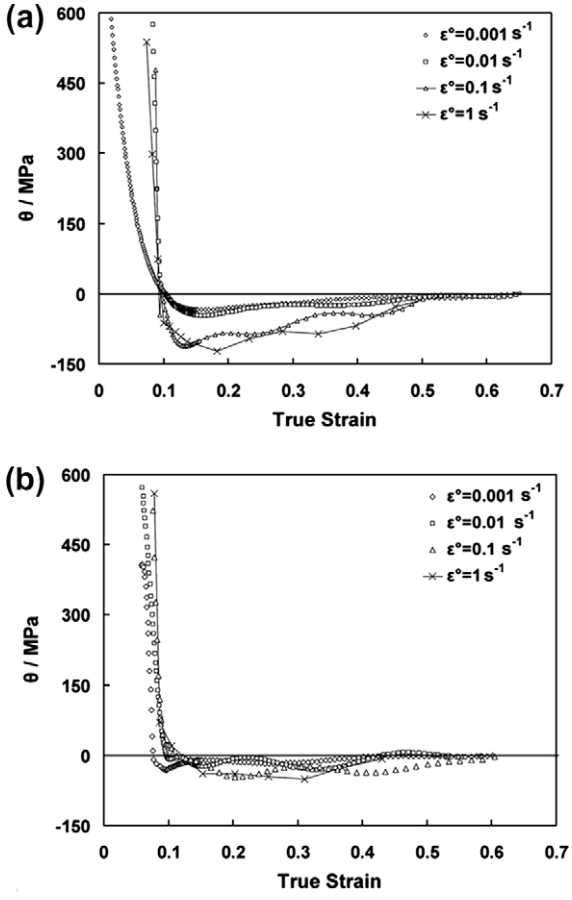

Fig. 7. Variation of work hardening rate with strain at (a) 950 °C, (b) 1000 °C and different strain rates.

mated value of $n = 4.91$ for single phase β microstructure is in better accordance with the value obtained via calculation of the strain sensitivity factor, i.e. 5.1. Although, the linear relationship between $\ln Z$ and $\ln[\sinh(A'\sigma)]$ shows that constitutive equation of hyperbolic sine function is valid for both microstructural regions, but it is better confirmed for hot deformation in single phase β region. This result may consolidate the idea that β undergoes DRX at high temperature deformations whereas the mixture of α + β softens by the phase transformation of α to β as well as what is so-called globularization.

The peak strain, ε_p, and thereby corresponding stress, σ_p, for initiation of flow softening in both single phase and two phase regions can be determined by depicting the variation of work hardening rate ($\theta = d\sigma/d\varepsilon$) versus true strain, Fig. 7. The parameter θ, which is obviously rendered as the tangent of flow curve at a given strain, increases primarily to a maximum followed by a linear decrease towards zero. While the material is prone to undergo dynamic recrystallization, such as β-phase, the curve of θ versus flow stress descends linearly to the stress which is the onset of subgrains formation [26]. Afterwards, the slope of this curve gradually decreases towards $\theta = 0$ at peak stress.

It is worth noting, at Fig. 7a all of curves reach zero at a fixed point which reflects the peak strain. Therefore, unlike to a material undergoing DRX, it can be seen that the peak strain for initiation of flow softening in α + β two phase region is almost independent to strain rate and to Z parameter as well. Otherwise, with respect to single phase β region the curves reach zero at different strains and therefore peak strain indicates dependence to Z, Fig. 7b. As the minimum amount of work hardening is accompanied by the maximum amount of flow softening, the minimums in Fig. 7 are associated with the highest rate of softening. The strain required for the highest rate of softening, ε^*, is a characteristic point in a typical flow curve of DRX. Fig. 8 exhibits the effect of temperature compensated strain rate, Z, on ε_p and ε^*.

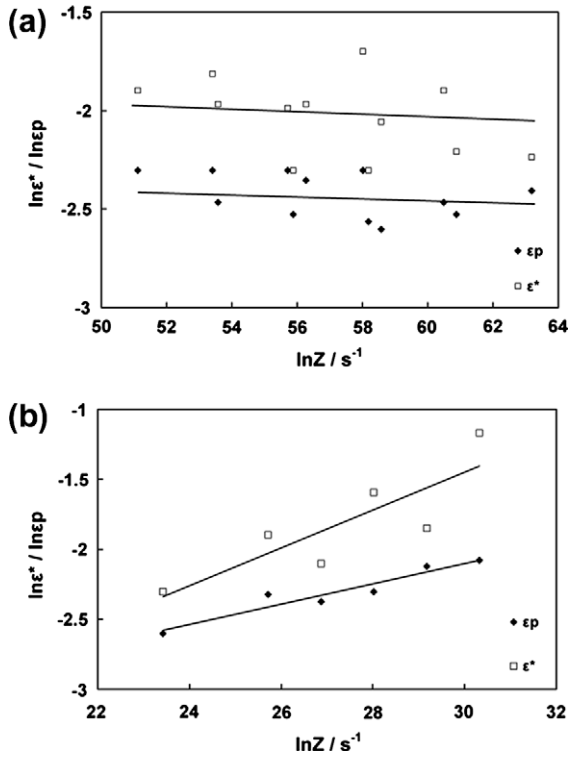

Fig. 8. The dependence of peak strain, ε_p, and the strain required for maximum amount of flow softening, ε^*, to Zenner–Hollomon parameter, Z, in (a) α + β and (b) β regions.

It is obviously seen that in two phase region both characteristic strains have a little or no dependence on Z. This is another reason for occurrence of a phase transformation as a softening mechanism in this case. Besides, the little difference between the values of ε_p and ε^* in Fig. 8 is attributed to the fact that the transformation of α to β and also globularization of α-phase take place more rapidly at early stages of softening period, perhaps similar to a site saturation mechanism. On the other hand, in single phase β region both ε_p and ε^* depend on processing parameters and corresponding relationships are proposed as follows:

$$\varepsilon_p = 1.4 \times 10^{-2} Z^{0.073} \tag{7}$$

$$\varepsilon^* = 4 \times 10^{-3} Z^{0.136} \tag{8}$$

The similar relationships have well developed and documented for other alloys such as stainless steels that undergo DRX [26–28].

4. Conclusions

1. The apparent differences of flow stress curves were analyzed in term of different dependence of flow stress to temperature and strain rate in both microstructural conditions. Therefore, the values of strain rate sensitivity, m, stress exponent, n and apparent activation energy, Q were assessed respectively as 0.2, 5 and 530 kJ/mol for two phase microstructure. For single phase β microstructure the aforementioned empirical constants were approximated 0.19, 5.1 and 376 kJ/mol, respectively.
2. The validity of constitutive equation of hyperbolic sine law was studied in both starting microstructures and it was concluded that the hot deformation behavior of β-phase is better fitted to this equation.
3. The values of strain corresponding to peak point, ε_p, and the highest rate of flow softening, ε^*, were determined by analyzing the variation of work hardening rate, θ, with true strain. It was found that in two phase region the characteristic strains are almost independent to Zenner–Hollomon parameter. In single phase region, ε_p and ε^* exhibited strong relationships with Z parameter and corresponding equations were proposed.

References

[1] Donelan P. Modeling microstructural and mechanical properties of ferritic ductile cast iron. Mater Sci Technol 2000;16:261–9.
[2] Osório WR, Garcia A. Modeling dendritic structure and mechanical properties of Zn–Al alloys. Mater Sci Eng 2002;325A:103–11.
[3] Lin DJ, Chuang CC, Lin JHC, Lee JW, Ju CP, Yin HS. Bone formation at the surface of low modulus Ti–7.5Mo implants in rabbit femur. Biomaterial 2007;28:2582–9.
[4] Cremasco A, Osório WR, Freire CMA, Garcia A, Caram R. Electrochemical corrosion behavior of a Ti–35Nb alloy for medical prostheses. Electrochim Acta 2008;53:4867–74.
[5] Moiseyev VN. Titanium alloys: Russian aircraft and aerospace applications. CRC Press Taylor & Francis Group; 2006. p. 169–80.
[6] Seshacharyulu T, Medeiros SC, Morgan JT, Malas JC, Frazier WG, Prasad YVRK. Hot deformation and microstructural damage mechanisms in extra-low interstitial (ELI) grade Ti–6Al–4V. Mater Sci Eng 2000;A279:289–99.
[7] Semiatin SL, Bieler TR. Effect of texture and slip mode on the anisotropy of plastic flow and flow softening during hot working of Ti–6Al–4V. Metals Mater Trans 2001;32A:1787–99.
[8] Seshacharyulu T, Medeiros SC, Frazier WG, Prasad YVRK. Hot working of commercial Ti–6Al–4V with an equiaxed α/β microstructure: materials modeling considerations. Mater Sci Eng 2000;A284:184–94.
[9] Seshacharyulu T, Medeiros SC, Frazier WG, Prasad YVRK. Microstructural mechanisms during hot working of commercial grade Ti–6Al–4V with lamellar starting structure. Mater Sci Eng 2002;A325:112–25.
[10] Semiantin SL, Bieler R. The effect of alpha platelet thickness on plastic flow during hot working of Ti–6Al–4V with a transformed microstructure. Acta Mater 2001;49:3565–73.
[11] Bruschi S, Poggio S, Quadrini F, Tata ME. Workability of Ti–6Al–4V alloy at high temperatures and strain rates. Mater Lett 2004;58:3622–9.

[12] Majorell A, Srivasta S, Picu RC. Mechanical behavior of Ti–6Al–4V at high and moderate temperatures-part1: experimental study. Mater Sci Eng 2002;A326:297–305.
[13] Warchomicka F, Stockinger M, Degischer HP. Quantitative analysis of the microstructure of near β titanium alloy during compression tests. J Mater Process Technol 2006;177:473–7.
[14] Cui WF, Jin Z, Guo AH, Zhou L. High temperature deformation behavior of α + β type biomedical titanium alloy Ti–6Al–7Nb. Mater Sci Eng 2009;A499: 252–6.
[15] Luo J, Li M, Li H, Yu W. Effect of the strain on the deformation behavior of isothermally compressed Ti–6Al–4V alloy. Mater Sci Eng 2009;505:88–95.
[16] Ding R, Guo ZX, Wilson A. Microstructural evolution of a Ti–6Al–4V alloy during thermomechanical processing. Mater Sci Eng 2002;A327:233–45.
[17] Hu ZM, Dean TA. Aspects of forging of titanium alloys and the production of blade forms. J Mater Process Technol 2001;111:10–9.
[18] Park NK, Yeom JT, Na YS. Characterization of deformation stability in hot forging of conventional Ti–6Al–4V using processing maps. J Mater Process Technol 2002;130–131:540–5.
[19] Kim JH, Semiatin SL, Lee CS. Constitutive analysis of the high temperature deformation mechanisms of Ti–6Al–4V and Ti–6.85Al–1.6V alloys. Mater Sci Eng 2005;A394:366–75.
[20] Li MQ, Zhang WF. Effect of hydrogen on processing maps in isothermal compression of Ti–6Al–4V titanium alloy. Mater Sci Eng 2009;A502(1–2):32–7.
[21] Lutjering G, Williams JC. Titanium. 2nd ed. New York: Springer; 2007. p. 23–8.
[22] Humphreys FJ, Hatherly M. Recrystallization and related annealing phenomena. 2nd ed. Netherland: Pergamon; 2004. p. 417.
[23] Farnoush H, Momeni A, Dehghani K, Aghazadeh Mohandesi J, Keshmiri H. Hot deformation characteristics of 2205 duplex stainless steel based on the behavior of constituent phases. Mater Des 2010;31:220–6.
[24] Tangerila S, Chaudhury PK, Zhao D, Valencia JJ. Hot deformation behavior of Ti–6Al–4V (ELI) alloy. In: Proceedings of the conference on advanced in hot deformation texture and microstructures, Materials week in Pittsburgh. October 18–20. TMS and ASM international; 1993.
[25] Sellars CM, Mc WJ, Tegart G. Hot workability. Int Metall Rev 1972;17:1.
[26] Cho SH, Yoo YC. Hot rolling simulation of austenitic stainless steel. J Mater Sci 2001;36:4267–72.
[27] Momeni A, Abbasi SM, Shokuhfar A. Dynamic recrystallization of a Cr–Ni–Mo–Cu–Ti–V precipitation hardenable stainless steel. J Mater Sci Technol 2007;23(6):775–8.
[28] Momeni A, Abbasi SM, Shokuhfar A. Hot compression behavior of as-cast precipitation–hardening stainless steel. J Iron Steel Res Int 2007;14(5):66–70.